Acta Crystallographica Section C
Crystal Structure Communications
ISSN 0108-2701

Two pentadehydropeptides with different configurations of the ΔPhe residues

Maciej Makowski,[a] Marek Lisowski,[b]* Anna Maciąg,[b] Maciej Wiktor,[b] Anna Szlachcic[b] and Tadeusz Lis[b]

[a]Institute of Chemistry, University of Opole, 48 Oleska Street, 45-052 Opole, Poland, and [b]Faculty of Chemistry, University of Wrocław, 14 Joliot-Curie Street, 50-383 Wrocław, Poland
Correspondence e-mail: mbl@wchuwr.pl

Received 16 December 2009
Accepted 25 January 2010
Online 3 February 2010

Comparison of the crystal structures of two pentadehydropeptides containing ΔPhe residues, namely (*Z*,*Z*)-*N*-(*tert*-butoxycarbonyl)glycyl-α,β-phenylalanylglycyl-α,β-phenylalanylglycine (or Boc^0–Gly^1–Δ^ZPhe^2–Gly^3–Δ^ZPhe^4–Gly^5–OH) methanol solvate, $C_{29}H_{33}N_5O_8 \cdot CH_4O$, (I), and (*E*,*E*)-*N*-(*tert*-butoxycarbonyl)glycyl-α,β-phenylalanylglycyl-α,β-phenylalanylglycine (or Boc^0–Gly^1–Δ^EPhe^2–Gly^3–Δ^EPhe^4–Gly^5–OH), $C_{29}H_{33}N_5O_8$, (II), indicates that the Δ^ZPhe residue is a more effective inducer of folded structures than the Δ^EPhe residue. The values of the torsion angles φ and ψ show the presence of two type-III′ β-turns at the Δ^ZPhe residues and one type-II β-turn at the Δ^EPhe residue. All amino acids are linked *trans* to each other in both peptides. β-Turns present in the peptides are stabilized by intramolecular 4→1 hydrogen bonds. Molecules in both structures form two-dimensional hydrogen-bond networks parallel to the (100) plane.

Comment

α,β-Dehydroamino acid residues contain a double bond between the C_α and C_β atoms. Due to this structural feature they have the capacity to induce ordered structures in peptides. These structures depend on the type, content and mutual location of Δ-amino acid residues in the peptide sequence. The conformation-stabilizing effect is very pronounced in the case of the ΔPhe residue. The presence of one or more ΔPhe residues results in the β-turn conformation in short peptides (Główka *et al.*, 1987; Główka, 1988; Aubry *et al.*, 1984) and the 3_{10} helical arrangement in longer peptides (Rajashankar *et al.*, 1992; Padmanabhan & Singh, 1993; Rajashankar, Ramakumar, Jain & Chauhan, 1995; Rajashankar, Ramakumar, Mal *et al.*, 1995; Jain *et al.*, 1997). The preferred values for the torsion angles φ and ψ fall predominantly into the regions of 80 and 0, 60 and 140, and 60 and 30°, respectively, and their enantiomeric values (Singh & Kaur, 1996).

This paper follows previous research on the conformational preferences of ΔPhe residues (Makowski *et al.*, 2006, and references therein). We present the structures of two pentadehydropeptides with two ΔPhe residues, *viz.* Boc^0–Gly^1–Δ^ZPhe^2–Gly^3–Δ^ZPhe^4–Gly^5–OH, (I), and Boc^0–Gly^1–Δ^EPhe^2–Gly^3–Δ^EPhe^4–Gly^5–OH, (II). The peptides differ only in the configuration of the ΔPhe residues. Both peptides crystallize in the same space group, $P2_1/c$, with one molecule in the asymmetric unit. Additionally, peptide (I) cocrystallizes with one molecule of methanol in the asymmetric unit. A comparison of the crystal structures of both peptides will allow evaluation of the impact of individual ΔPhe isomers on the conformational preferences of the peptides. The atom labelling is the same in both structures.

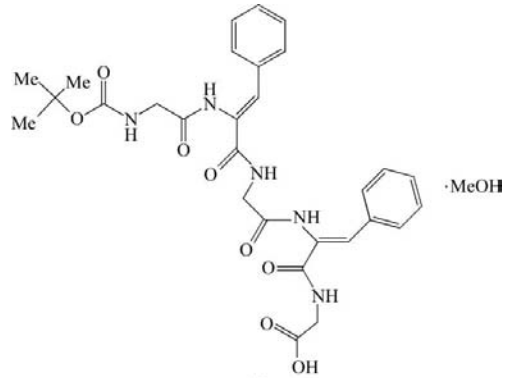

(I)

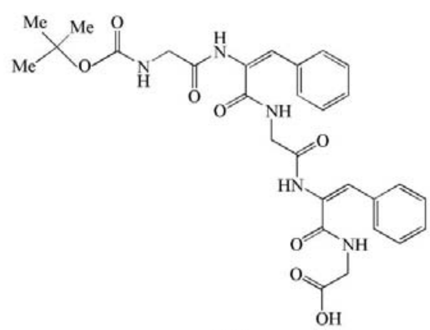

(II)

All amino acids, in both structures, are linked *trans* to each other. The deviations from ideal ω = 180° do not exceed 10°. Blocking groups adopt *transoidal* conformations, as indicated by the values of the ω^0 (N1—C5—O1—C1) and φ^0 (C6—N1—C5—O1) torsion angles (Tables 1 and 3). The C_α—C_β distances (C8═C9 and C19═C20) are classical double-bond lengths (Tables 1 and 3) and correspond well with the results of other X-ray crystallographic studies of dehydropeptides (Główka *et al.*, 1987; Ejsmont *et al.*, 2001; Makowski *et al.* 2005).

Because of the unsaturated character of the C_α—C_β bond, the side chains of the ΔPhe residues are much closer to the main-chain atoms compared with their saturated counterparts. This feature results in some geometric distortions characteristic of dehydropeptide structures (Główka *et al.*, 1987). Systematic shortening of the N—C_α (N2—C8 and N4—C19), C_α—C_β (C8—C16 and C19—C27) and C_β—C_γ (C9—C10 and

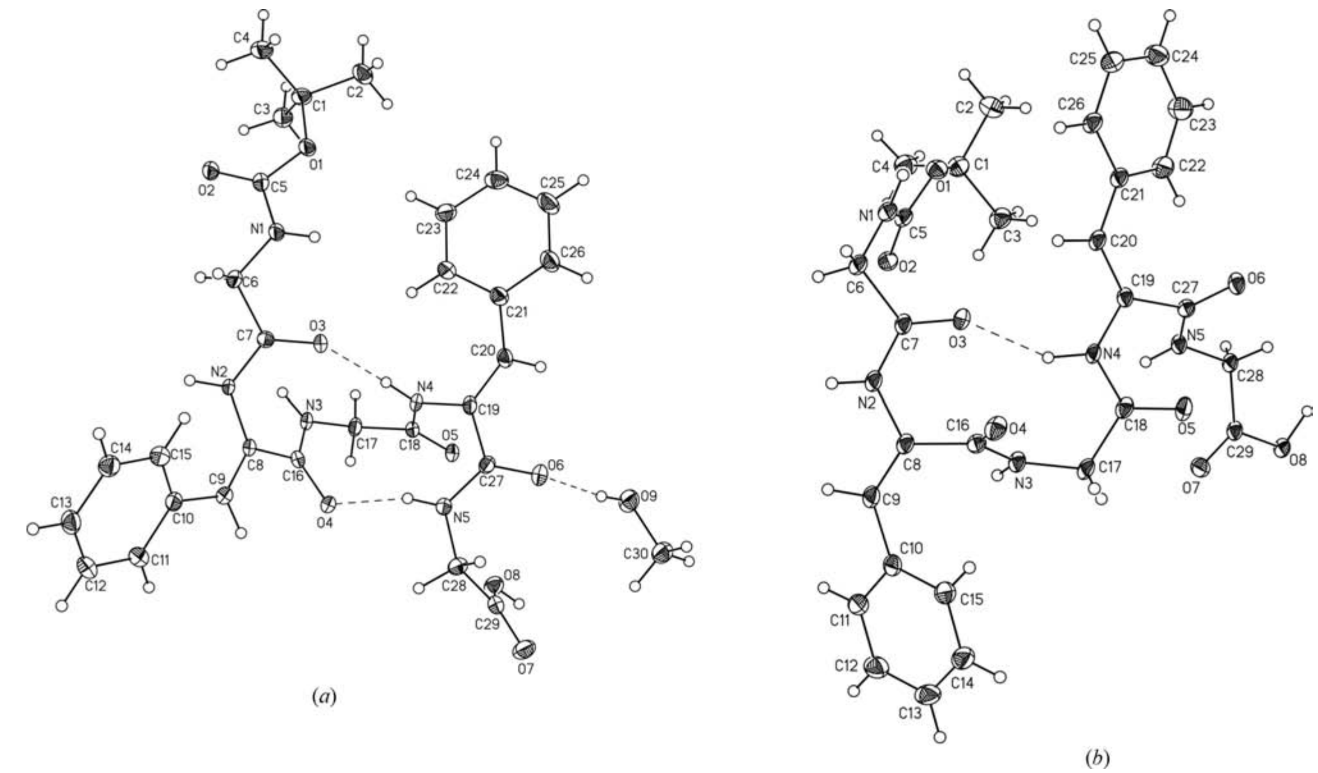

Figure 1
The molecular structures of peptides (*a*) (I) and (*b*) (II), showing the atom-numbering schemes. Displacement ellipsoids are drawn at the 30% probability level and H atoms are shown as small spheres of arbitrary radii. Hydrogen bonds are shown as dashed lines.

C20—C21) single bonds (Tables 1 and 3) is observed, which may be caused by extended delocalization of the π electron system. The values of the N2—C8—C16 [118.8 (2) and 114.67 (18)° for (I) and (II), respectively] and N4—C19—C27 [117.1 (2) and 114.04 (18)° for (I) and (II), respectively] bond angles are smaller than the regular trigonal value of 120°, which is clearly understandable owing to the steric interactions between the main chain and the side chains of ΔPhe. It is interesting that these effects influence analogous angles in both peptides to the same extent, regardless of the location of the aromatic rings.

Another characteristic consequence of the short distance between the aromatic rings and the peptide chain is a considerable opening of the valence angles $C_\alpha—C_\beta—C_\gamma$ to relax the steric strain (Główka, 1988). This trend explains the increased values of the $C_\alpha—C_\beta—C_\gamma$ bond angles for both structures. These angles are the same in both ΔPhe residues in each structure and agree to within one standard deviation between (I) and (II). In the case of (I), these angles for Δ^ZPhe^2 and Δ^ZPhe^4 are C8—C9—C10 = 131.4 (3)° and C19—C20—C21 = 131.4 (3)°, respectively, and for Δ^EPhe^2 and Δ^EPhe^4 of (II) they are C8—C9—C10 = 129.9 (2)° and C19—C20—C21 = 129.9 (2)°, respectively. The torsion angles χ^2 = −176.9 (2)° and χ^4 = −176.0 (2)° between N—C$^\alpha$ and the aromatic system, and $\chi^{2,1}$ = −155.1 (3)°, $\chi^{2,2}$ = 25.4 (4)°, $\chi^{4,1}$ = 20.7 (4)° and $\chi^{4,2}$ = −159.7 (2)°, indicate that in the case of (II) the side chains of both ΔPhe residues are almost planar, while for (I) the torsion angles χ^4 = 0.2 (5)°, $\chi^{4,1}$ = −19.8 (5)° and $\chi^{4,2}$ = 162.9 (3)° show that only the side chain of ΔPhe^4 is planar. The ΔPhe^2 residue side chain adopts a *trans*-(−)*gauche* conformation, with torsion angles $\chi^{2,1}$ = −152.6 (3)° and $\chi^{2,2}$ = 30.8 (5)°.

The presence of two Δ^ZPhe residues in (I) induces the occurrence of two overlapping β-turns. The first is formed by the Δ^ZPhe^2 and Gly^3 residues, with torsion angles φ_2 = 50.4 (4)° and ψ_2 = 20.0 (4)°, and φ_3 = 54.7 (4)° and ψ_3 = 26.7 (4)°, respectively. The second turn includes the Gly^3 and Δ^ZPhe^4 residues, with torsion angles φ_3 = 50.4 (4)° and ψ_3 = 20.0 (4)°, and φ_4 = 68.7 (3)° and ψ_4 = 17.4 (4)°, respectively. The torsion angles indicate that these β-turns are of type III′ (Lewis *et al.*, 1973). They are stabilized by 4→1 hydrogen bonds between the NH group of Δ^ZPhe^4 and the CO group of Gly^1, and between the NH group of Gly^5 and the CO group of Δ^ZPhe^2 (Table 2). The two β-turns of type III′ in (I) are the same as in the previously reported crystal structure of the Boc^0–Gly^1–Δ^ZPhe^2–Gly^3–Δ^ZPhe^4–Gly^5–OMe pentapeptide, which differs from (I) only in the methanolate group at the C terminus (Makowski *et al.*, 2007). The molecular structure of peptide (I) is presented in Fig. 1(*a*) and its packing diagram is shown in Fig. 2.

The situation is somewhat different in the case of (II). There is only one β-turn at the Δ^EPhe^2 and Gly^3 residues, stabilized by a 4→1 hydrogen bond between the NH group of Δ^EPhe^4 and the CO group of Gly^1 (Table 4). This β-turn is additionally stabilized by a C—H$\cdots\pi$ interaction. The φ and ψ angles of these residues are 33.2 (3) and −119.6 (2)°, and −83.2 (3) and −5.3 (3)°, respectively. These values correspond well with a type-II β-turn (Lewis *et al.*, 1973). Deviations from the ideal

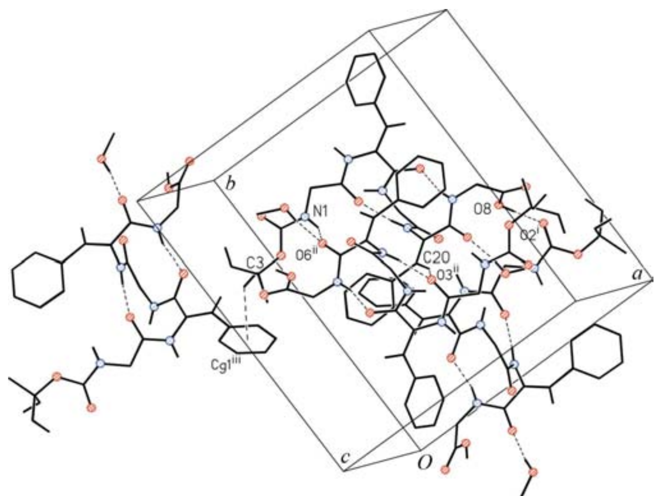

Figure 2
A packing diagram for peptide (I). Hydrogen bonds are represented by dashed lines. Symmetry codes are as given in Table 2.

torsion angles for this β-turn (−60 and 120°, and 80 and 0°) are not larger than 26°, compared with a maximum acceptable deviation of 40° (Lewis *et al.*, 1973). In addition, the C-terminal amino acid residues adopt a conformation similar to a type-IV β-turn. The whole structure is stabilized by inter- and intramolecular hydrogen bonds of various types, namely O—H$\cdots$O, N—H$\cdots$O and C—H$\cdots\pi$ (Table 4). However, the conformational constraints are not sufficient for a second β-turn to be formed. The molecular structure of peptide (II) is presented in Fig. 1(*b*).

A comparison of (I) and (II) reveals that a Δ^ZPhe residue is a more effective inducer of folded structures than a Δ^EPhe residue. The insertion of two Δ^ZPhe residues in (I) gives rise to the formation of two β-turns and the structure is stabilized by two intramolecular 4→1 hydrogen bonds. In the case of (II), there is only one β-turn stabilized by a hydrogen bond and the resulting conformation is more distorted, and this is reflected in the greater deviations from ideal dihedral angles for the β-turns. The previously reported crystal structure of a closely related peptide, *viz.* Boc–Gly–Δ^ZPhe–Gly–Δ^EPhe–Gly–OMe (Makowski *et al.*, 2006), shows that in the case of a Δ^EPhe^4 residue the formation of a second β-turn is hindered and deviations from ideal values for the torsion angles φ and ψ are increased. A type-II β-turn for the Δ^ZPhe^2 and Gly^3 residues, and a type-IV β-turn for Gly^3 and Δ^EPhe^4, was observed. The Δ^EPhe^4 residue in (II) does not induce a β-turn, as in the case of Boc^0–Gly^1–Δ^ZPhe^2–Gly^3–Δ^EPhe^4–Gly^5–OMe. A β-turn at the Δ^EPhe^4 residue has been observed for Boc^0–Gly^1–Δ^ZPhe^2–Gly^3–Δ^EPhe^4–Phe^5-*p*-NA·EtOH (Makowski *et al.*, 2005), due to the presence of the additional H-atom donor, *p*-nitroaniline (*p*-NA), which forms a hydrogen bond with the CO group of Gly^3.

The atypical location of the H atom of the C-terminal carboxyl group, H8, merits further discussion. In (II) it is directed to the opposite side compared with the analogous atom in (I). The O8 atoms in both molecules take part in hydrogen bonds. In the case of (II), atom H8 participates in the intermolecular N2—H2$\cdots$O8($1-x, y-\frac{1}{2}, \frac{1}{2}-z$) hydrogen bond (Table 4). The formation of this bond requires a relocation of the H atom. What is more, amide atom H2 of another molecule of (II) in that hydrogen bond corresponds to the position of the carboxyl H atom in (I). Therefore, we suspect some competition between the O8—H8 covalent bond and the N2—H2$\cdots$O8($1-x, y-\frac{1}{2}, \frac{1}{2}-z$) hydrogen bond which results in moving atom H8 to the alternative position.

Further information can be derived from a detailed analysis of the packing diagrams of both molecules. The crystal structure stabilizing effect compensates for the energy loss resulting from the unusual position of the H atom in (II). Additionally, the position of atom H8 in (II) is stabilized by the O8—H8$\cdots$O2($x, \frac{1}{2}-y, \frac{1}{2}+z$) hydrogen bond. This unusual position of the hydroxy H atom is rarely encountered. As reported recently, it occurs when additional stabilization is provided by other interactions (Videnova-Adrabinska *et al.*, 2007). In the discussed case, the H atom switches its orientation to approach the lone pair of another hydroxy O atom.

Experimental

Both title compounds were obtained from their methyl esters. The syntheses of the methyl esters of (I) and (II) have been described by Latajka *et al.* (2008). For the preparation of (I), Boc–Gly–Δ^ZPhe–Gly–Δ^ZPhe–Gly–OMe (0.059 g, 0.1 mmol) was dissolved in MeOH (1.5 ml) and then H_2O (0.1 ml) and 1 *M* NaOH (0.3 ml, 0.3 mmol) were added. The reaction was carried out for 30 min at room temperature. The reaction mixture was then acidified to pH 3 and brine (*ca* 10 ml) was added. The mixture was extracted with EtOAc (5 × 3 ml). The acetate extracts were washed with 0.5 *M* HCl (2 × 2 ml) and brine (2 × 2 ml) and dried over anhydrous $MgSO_4$. After removal of EtOAc in vacuo, Boc–Gly–Δ^ZPhe–Gly–Δ^ZPhe–Gly–OH was crystallized from EtOAc with addition of hexane to the first turbidity [yield 0.056 g, 97%; m.p. 474–477 K (decomposition)]. Elemental analysis calculated for $C_{29}H_{33}N_5O_8$: C 60.09, H 5.74, N 12.08%; found: C 59.89, H 5.98, N 12.12%. Boc–Gly–Δ^EPhe–Gly–Δ^EPhe–Gly–OH, (II), was obtained from its methyl ester in the same way [yield 0.054 g, 94%; m.p. 474–477 K (decomposition)]. Elemental analysis calculated for $C_{29}H_{33}N_5O_8$: C 60.09, H 5.74, N 12.08%; found: C 60.33, H 5.87, N 11.89%. Finally, peptide (II) were recrystallized from a solution in a mixture of MeOH and EtOAc.

Compound (I)

Crystal data

$C_{29}H_{33}N_5O_8\cdot CH_4O$
M_r = 611.65
Monoclinic, $P2_1/c$
a = 14.075 (4) Å
b = 16.577 (5) Å
c = 14.041 (4) Å
β = 112.34 (3)°
V = 3030.2 (17) Å^3
Z = 4
Cu $K\alpha$ radiation
μ = 0.84 mm^{-1}
T = 100 K
0.30 × 0.20 × 0.01 mm

Data collection

Oxford Xcalibur PX κ-geometry diffractometer with CCD area detector
Absorption correction: analytical [*CrysAlis RED* (Oxford Diffraction, 2003); analytical numeric absorption correction using a multifaceted crystal model based on the expressions derived by Clark & Reid (1995)]
T_{min} = 0.842, T_{max} = 0.966
22848 measured reflections
5247 independent reflections
3735 reflections with $I > 2\sigma(I)$
R_{int} = 0.099

Table 1
Selected geometric parameters (Å, °) for (I).

N2—C8	1.428 (3)	N4—C19	1.433 (4)
C8—C9	1.339 (4)	C19—C20	1.336 (4)
C8—C16	1.508 (4)	C19—C27	1.493 (4)
C16—O4	1.248 (3)	C27—O6	1.244 (3)
C9—C10	1.471 (4)	C20—C21	1.465 (4)
N2—C8—C16	118.8 (2)	N4—C19—C27	117.1 (2)
C8—C9—C10	131.4 (3)	C19—C20—C21	131.4 (3)
N1—C6—C7—N2	161.6 (2)	N3—C17—C18—N4	26.7 (4)
C6—C7—N2—C8	176.0 (3)	C17—C18—N4—C19	−175.6 (2)
C7—N2—C8—C16	50.4 (4)	C18—N4—C19—C27	68.7 (3)
N2—C8—C16—N3	20.0 (4)	N4—C19—C27—N5	17.4 (4)
N2—C8—C9—C10	5.8 (5)	C19—C27—N5—C28	177.7 (2)
C8—C9—C10—C11	−152.6 (3)	C27—N5—C28—C29	73.0 (4)
C8—C9—C10—C15	30.8 (5)	C6—N1—C5—O1	−179.9 (2)
C8—C16—N3—C17	−170.5 (2)	N1—C5—O1—C1	−171.3 (2)
C16—N3—C17—C18	54.7 (4)		

Table 2
Hydrogen-bond geometry (Å, °) for (I).

*Cg*1 is the centroid of the ring defined by atoms C21–C26.

D—H⋯*A*	*D*—H	H⋯*A*	*D*⋯*A*	*D*—H⋯*A*
O8—H8⋯O2^{i}	0.84	1.75	2.587 (3)	172
N1—H1⋯O6^{ii}	0.88	2.25	2.903 (3)	131
N4—H4⋯O3	0.88	1.99	2.860 (3)	168
N5—H5⋯O4	0.88	2.08	2.927 (3)	162
O9—H9*M*⋯O6	0.84	1.87	2.703 (3)	173
N1—H1⋯O3	0.88	2.38	2.691 (3)	101
N4—H4⋯N3	0.88	2.42	2.769 (3)	104
N5—H5⋯N4	0.88	2.43	2.788 (3)	105
C20—H20⋯O3^{ii}	0.95	2.45	3.246 (4)	141
C9—H9⋯O4	0.95	2.40	2.786 (4)	104
C3—H3*A*⋯O2	0.98	2.43	2.982 (4)	115
C4—H4*A*⋯O2	0.98	2.43	2.993 (4)	116
C3—H3*B*⋯*Cg*1^{iii}	0.98	2.94	3.735 (4)	138

Symmetry codes: (i) $-x+1, y-\frac{1}{2}, -z+\frac{1}{2}$; (ii) $-x+1, -y+1, -z+1$; (iii) $x-1, -y+\frac{3}{2}, z-\frac{1}{2}$.

Table 3
Selected geometric parameters (Å, °) for (II).

O4—C16	1.229 (3)	C8—C16	1.500 (3)
O6—C27	1.228 (3)	C9—C10	1.472 (3)
N2—C8	1.422 (3)	C19—C20	1.338 (3)
N4—C19	1.408 (3)	C19—C27	1.512 (3)
C8—C9	1.324 (3)	C20—C21	1.462 (3)
N2—C8—C16	114.67 (18)	N4—C19—C27	114.04 (18)
C8—C9—C10	129.9 (2)	C19—C20—C21	129.9 (2)
C1—O1—C5—N1	179.64 (19)	C8—C9—C10—C11	−155.1 (3)
C6—N1—C5—O1	−170.52 (18)	C16—N3—C17—C18	−83.2 (3)
C8—N2—C7—C6	176.33 (19)	C19—N4—C18—C17	−172.19 (19)
N1—C6—C7—N2	−163.93 (18)	N3—C17—C18—N4	−5.3 (3)
C7—N2—C8—C16	33.2 (3)	C18—N4—C19—C27	35.8 (3)
C17—N3—C16—C8	−175.0 (2)	C28—N5—C27—C19	−174.9 (2)
N2—C8—C16—N3	−119.6 (2)	N4—C19—C27—N5	55.4 (3)
N2—C8—C9—C10	−176.9 (2)	C27—N5—C28—C29	122.3 (2)
C8—C9—C10—C15	25.4 (4)		

Table 4
Hydrogen-bond geometry (Å, °) for (II).

*Cg*1 is the centroid of the ring defined by atoms C21–C26.

D—H⋯*A*	*D*—H	H⋯*A*	*D*⋯*A*	*D*—H⋯*A*
N4—H4⋯O3	0.88	2.07	2.867 (2)	150
O8—H8⋯O2^{i}	0.84	1.76	2.602 (3)	177
N2—H2⋯O8^{ii}	0.88	2.12	2.926 (2)	152
N1—H1⋯O4^{iii}	0.88	1.93	2.782 (2)	163
N5—H5⋯O6^{iv}	0.88	2.01	2.886 (3)	178
N3—H3⋯O5^{iv}	0.88	1.99	2.721 (2)	139
C2—H2*C*⋯*Cg*1	0.98	2.87	3.851 (4)	176
C28—H28*B*⋯*Cg*1^{iv}	0.99	2.81	3.647 (3)	142

Symmetry codes: (i) $x, -y+\frac{1}{2}, z+\frac{1}{2}$; (ii) $-x+1, y-\frac{1}{2}, -z+\frac{1}{2}$; (iii) $-x+1, -y, -z+1$; (iv) $x, -y+\frac{1}{2}, z-\frac{1}{2}$.

Refinement

$R[F^2 > 2\sigma(F^2)] = 0.070$
$wR(F^2) = 0.205$
$S = 1.03$
5247 reflections
404 parameters
H-atom parameters constrained
$\Delta\rho_{max} = 0.42$ e Å^{-3}
$\Delta\rho_{min} = -0.39$ e Å^{-3}

Compound (II)

Crystal data

$C_{29}H_{33}N_5O_8$
$M_r = 579.60$
Monoclinic, $P2_1/c$
$a = 13.520$ (6) Å
$b = 22.9220$ (11) Å
$c = 9.795$ (5) Å
$\beta = 97.41$ (5)°
$V = 3010$ (2) Å^3
$Z = 4$
Cu $K\alpha$ radiation
$\mu = 0.79$ mm^{-1}
$T = 100$ K
0.38 × 0.25 × 0.04 mm

Data collection

Oxford Xcalibur PX κ-geometry diffractometer with CCD area detector
Absorption correction: analytical (*CrysAlis RED*; Oxford Diffraction, 2003)
$T_{min} = 0.760$, $T_{max} = 0.970$
24796 measured reflections
5975 independent reflections
3955 reflections with $I > 2\sigma(I)$
$R_{int} = 0.065$

Refinement

$R[F^2 > 2\sigma(F^2)] = 0.053$
$wR(F^2) = 0.140$
$S = 1.00$
5975 reflections
383 parameters
H-atom parameters constrained
$\Delta\rho_{max} = 0.40$ e Å^{-3}
$\Delta\rho_{min} = -0.35$ e Å^{-3}

H atoms bonded to C atoms were placed in geometrically optimized positions and treated as riding, with C—H = 0.95 (aromatic), 0.98 (methyl) or 0.99 Å (methylene). H atoms belonging to the amide and hydroxy groups were initially located in difference Fourier maps and in the final refinement their positions were geometrically optimized and treated as riding, with N—H = 0.88 Å and O—H = 0.84 Å. For all H atoms except the methyl groups of (II), U_{iso}(H) = 1.2U_{eq}(C,N,O). For the methyl groups of (II), U_{iso}(H) = 1.5U_{eq}(C).

For both compounds, data collection: *CrysAlis CCD* (Oxford Diffraction, 2003); cell refinement: *CrysAlis RED* (Oxford Diffraction, 2003); data reduction: *CrysAlis RED*; program(s) used to solve structure: *SHELXS97* (Sheldrick, 2008); program(s) used to refine structure: *SHELXL97* (Sheldrick, 2008). Molecular graphics: *XP* in *SHELXTL* (Sheldrick, 2008) for (I); *Mercury* (Macrae *et al.*, 2006) and *SHELXTL* for (II). For both compounds, software used to prepare material for publication: *SHELXL97*.

Supplementary data for this paper are available from the IUCr electronic archives (Reference: SK3358). Services for accessing these data are described at the back of the journal.

References

Aubry, A., Boussard, G. & Marraud, M. (1984). *C. R. Acad. Sci. Ser. II*, **299**, 1031–1033.

Clark, R. C. & Reid, J. S. (1995). *Acta Cryst.* A**51**, 887–897.

Ejsmont, K., Makowski, M. & Zaleski, J. (2001). *Acta Cryst.* C**57**, 205–207.

Główka, M. L. (1988). *Acta Cryst.* C**44**, 1639–1641.

Główka, M. L., Gilli, G., Bertolasi, V. & Makowski, M. (1987). *Acta Cryst.* C**43**, 1403–1406.

Jain, R. M., Rajashankar, K. R., Ramakumar, S. & Chauhan, V. S. (1997). *J. Am. Chem. Soc.* **119**, 3205–3211.

Latajka, R., Jewginski, M., Makowski, M., Pawełczak, M., Huber, T., Sewald, N. & Kafarski, P. (2008). *J. Pept. Sci.* **14**, 1084–1095.

Lewis, P. N., Momany, F. A. & Scheraga, H. A. (1973). *Biochim. Biophys. Acta*, **303**, 211–229.

Macrae, C. F., Edgington, P. R., McCabe, P., Pidcock, E., Shields, G. P., Taylor, R., Towler, M. & van de Streek, J. (2006). *J. Appl. Cryst.* **39**, 453–457.

Makowski, M., Brzuszkiewicz, A., Lisowski, M. & Lis, T. (2005). *Acta Cryst.* C**61**, o424–o426.

Makowski, M., Lisowski, M., Maciąg, A. & Lis, T. (2006). *Acta Cryst.* E**62**, o807–o810.

Makowski, M., Lisowski, M., Mikołajczyk, I. & Lis, T. (2007). *Acta Cryst.* E**63**, o989–o991.

Oxford Diffraction (2003). *CrysAlis CCD* and *CrysAlis RED*. Versions 1.171. Oxford Diffraction, Wrocław, Poland.

Padmanabhan, B. & Singh, T. P. (1993). *Biopolymers*, **33**, 613–619.

Rajashankar, K. R., Ramakumar, S. & Chauchan, V. S. (1992). *J. Am. Chem. Soc.* **114**, 9225–9226.

Rajashankar, K. R., Ramakumar, S., Jain, R. M. & Chauhan, V. S. (1995). *J. Am. Chem. Soc.* **117**, 11773–11779.

Rajashankar, K. R., Ramakumar, S., Mal, T. K., Jain, R. M. & Chauhan, V. S. (1995). *Biopolymers*, **35**, 141–147.

Sheldrick, G. M. (2008). *Acta Cryst.* A**64**, 112–122.

Singh, T. P. & Kaur, P. (1996). *Prog. Biophys. Mol. Biol.* **66**, 141–165.

Videnova-Adrabinska, V., Obara, E. & Lis, T. (2007). *New J. Chem.* **31**, 287–295.